Award Number: 04HQGR0008

GEODETIC MEASUREMENTS FOR URBAN EARTHQUAKE HAZARD IN SAN DIEGO, CALIFORNIA: THE ROSE CANYON FAULT ZONE

Final Technical Report July 1, 2007

Duncan Carr Agnew

Institute of Geophysics and Planetary Physics
Scripps Institution of Oceanography
University of California, San Diego
La Jolla, CA 92093-0225
(858) 534-2590 (FAX 534-5332); dagnew@ucsd.edu

Award Number: 04HQGR0008

GEODETIC MEASUREMENTS FOR URBAN EARTHQUAKE HAZARD IN SAN DIEGO, CALIFORNIA: THE ROSE CANYON FAULT ZONE

Final Technical Report July 1, 2007

Duncan Carr Agnew

Institute of Geophysics and Planetary Physics
Scripps Institution of Oceanography
University of California, San Diego
La Jolla, CA 92093-0225
(858) 534-2590 (FAX 534-5332); dagnew@ucsd.edu

Abstract

This grant funded remeasurement of a GPS network spanning the Rose Canyon fault, an active fault running through the heart of urban San Diego. Measuring the motions of points in this network between our first survey in 1998, and later, will show us how much motion is occurring at depth across this fault—motion that would someday be released in an earthquake. These measurements thus provide information to improve estimates of the seismic hazard and risk from the Rose Canyon fault zone. Results from processing the baselines for the individual monument clusters in the network show measurement error of 0.3 mm and random walk of about 0.3 mm over a year; analysis of time series of data from new continuous stations shows higher strain rates (north-south contraction) close to the Rose Canyon fault and smaller rates inland.

Accomplishments: Investigations Undertaken, Results

1. Introduction

This grant supported remeasurement of a GPS network spanning the Rose Canyon fault, an active fault running through the heart of urban San Diego. Geological estimates of the rate of motion on this fault are about 1–2 mm/yr; however, this rate comes from trenching at a single site, which may not span the entire fault zone, and the geometry of the fault system is poorly understood to the south of San Diego, in part because it crosses both the coastline and the international border. Geodetic measurements can help to elucidate both the geometry and the rate of motion; those collected so far suggest a higher rate of motion, 3-4 mm/yr, across the greater San Diego area.

1.1. Survey-mode Measurements: Monument Clusters

In 1998, with NEHRP support, we constructed four high-precision "GPS clusters": multiple monuments in stable material, spaced from 30 to 400 m apart; to go with these we built special equipment to center GPS antennas over these points to 0.2 mm repeatability. **Figure 1** shows the locations of these clusters.

1.1.1. Rationale for Monument Clusters

The reason for these clusters was to decrease the level of monument-related noise by averaging over multiple locations: an alternative to deep-braced monuments. This development derives from studies (by

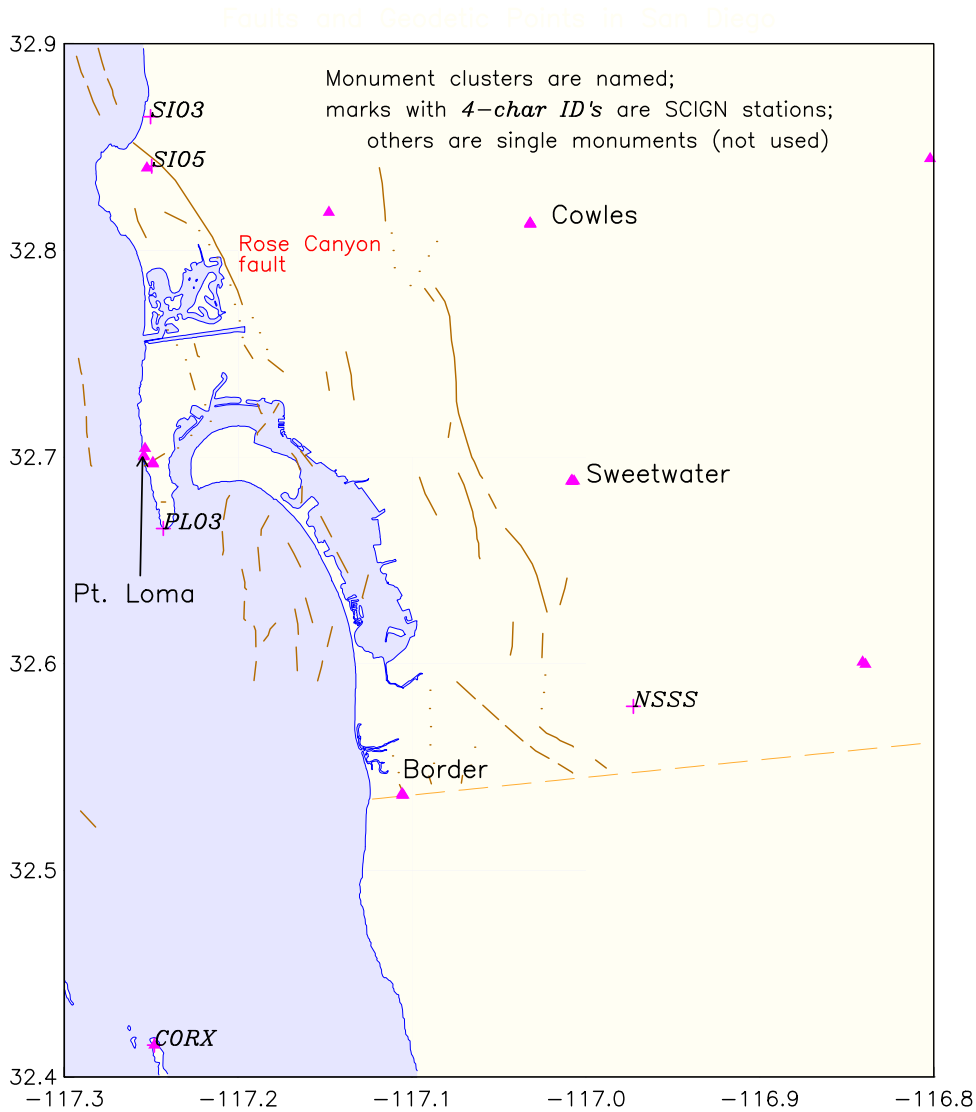

Figure 1

ourselves and others: Langbein and Johnson 1997; Zhang *et al.* 1997; Mao *et al.* 1999) of noise in GPS and EDM time series. These show increasing energy at low frequencies, usually best represented as one or more power-law processes (power spectral density varying as $f^{-\alpha}$ with α between 1 (flicker noise) and 2 (a random walk)). As noted by Johnson and Agnew (1995), such behavior implies that the errors in estimating a rate (velocity) are much larger than would be the case if the noise was independent between observations ($\alpha = 0$, or white noise); if a random walk process is dominant the velocity uncertainty is approximately $\sigma_{vel} = \sigma_{RW}/\sqrt{T}$ where σ_{RW} is the amplitude of the random walk noise (in mm/$\sqrt{\text{year}}$) and T is the total duration of the measurements in years; the number and spacing of measurements is immaterial to first order. To measure the expected motion on the Rose Canyon Fault (1.5±0.5 mm/yr) we need errors in velocity of better than ±0.7 mm/yr. Using the expression above we can determine an appropriate experiment duration for any level of velocity-uncertainty if we know a value for σ_{RW}. Langbein and Johnson (1997) found pier-type monuments to show an average σ_{RW} of about 1.3 mm/$\sqrt{\text{year}}$; then if T is 5 years, $\sigma_{vel} = 0.6$ mm/yr, with a 95% confidence ellipse of about ±1.4 mm/yr. To decrease the error we could either extend T to 20 years, or reduce σ_{RW}. The best (though costly) way to do this is to build, as SCIGN

and PBO have, deep-braced monuments; as a cheaper alternative, we decided to use multiple monuments. This second approach also makes the survey more robust over time, since destruction of an individual monument does not then mean that the site is lost. If, as appears to be true, the individual monuments of a cluster move independently, then measurements to N monuments will reduce σ_{RW} by $N^{-\frac{1}{2}}$: four monuments will cut the error in half.

Of course, to get realistic errors requires that we know σ_{RW} for the monuments. This usually requires a long time series with many points; but this requirement comes mostly from the need to establish the complete spectrum—which in turn is needed because of the relatively large white-noise and flicker-noise components in GPS time series. But with a monument cluster these components are very much reduced, because over baselines of 100 meters GPS can be used with much higher accuracy, free from atmospheric effects and reference-frame problems. Effectively, the inter-cluster distances can be measured very accurately and the stability of each mark determined.

1.1.2. High-Precision Fixed-Height Antenna Mount

To take advantage of this very high accuracy of GPS over short distances we must be able to position an antenna above the actual mark on the ground to sub-mm accuracy: something not possible with a tripod and optical plummet. We designed a high-precision fixed-height antenna post that is kinematically positioned on the mark. The antenna post is a large-diameter precision-ground stainless steel rod. This is held in place by three adjustable chains which attach to a spring-loaded collar on the post—this introduces some (intentional) elasticity into the setup so that slight variations in force cannot induce permanent deformation. The post is set vertically using turnbuckles to adjust the length of each chain; once this is done the turnbuckles are locked in place. Most fixed-height antenna mounts use levels permanently attached to the mount; but these will be affected by any bending of the post. We instead use a separate leveling system, with very sensitive bubble levels. This is clamped to the post during setup, and can be rotated around the post to verify verticality and check its own calibration (by rotating it through 180°). While this style of setup is initially more difficult than for a typical tripod, after some training it can be done as easily—and almost 10 times more accurately. In tests in our lab (using a micrometer mounted on a milling machine as a check) we find that different people can independently set up this equipment to better than 0.1 mm repeatability.

The ground monuments are 2″-diameter stainless-steel plugs set in drilled holes in solid rock or concrete. These plugs each have an internally-threaded cap in the top; this cap can be removed using a specially designed wrench (to prevent tampering) and has a center mark machined into its surface (so it can be used with conventional survey equipment). For use with the fixed-height post the cap is removed and another insert screwed in; this insert has a cone-shaped depression that mates kinematically (and hence uniquely) to a hemispherical base on the bottom of the post. If either piece is damaged it can be removed and easily replaced with a duplicate. The hold-down chains are attached to the ground and 3 points, each about 2 feet away from the central mark; these points are threaded inserts that accept an eye-bolt when surveying; when not in use the eye-bolts are replaced by allen-head bolts.

1.1.3. Cluster Siting and Construction

After much searching for sites which would span the fault at which the surface material was competent enough to install the marks, we constructed five monument clusters, with locations shown in **Figure 1**; **Figure 2** shows plans of four of these, with topography (contour interval 1 m for all plots except for the Pt. Loma cluster, which is 5 m) The sites are

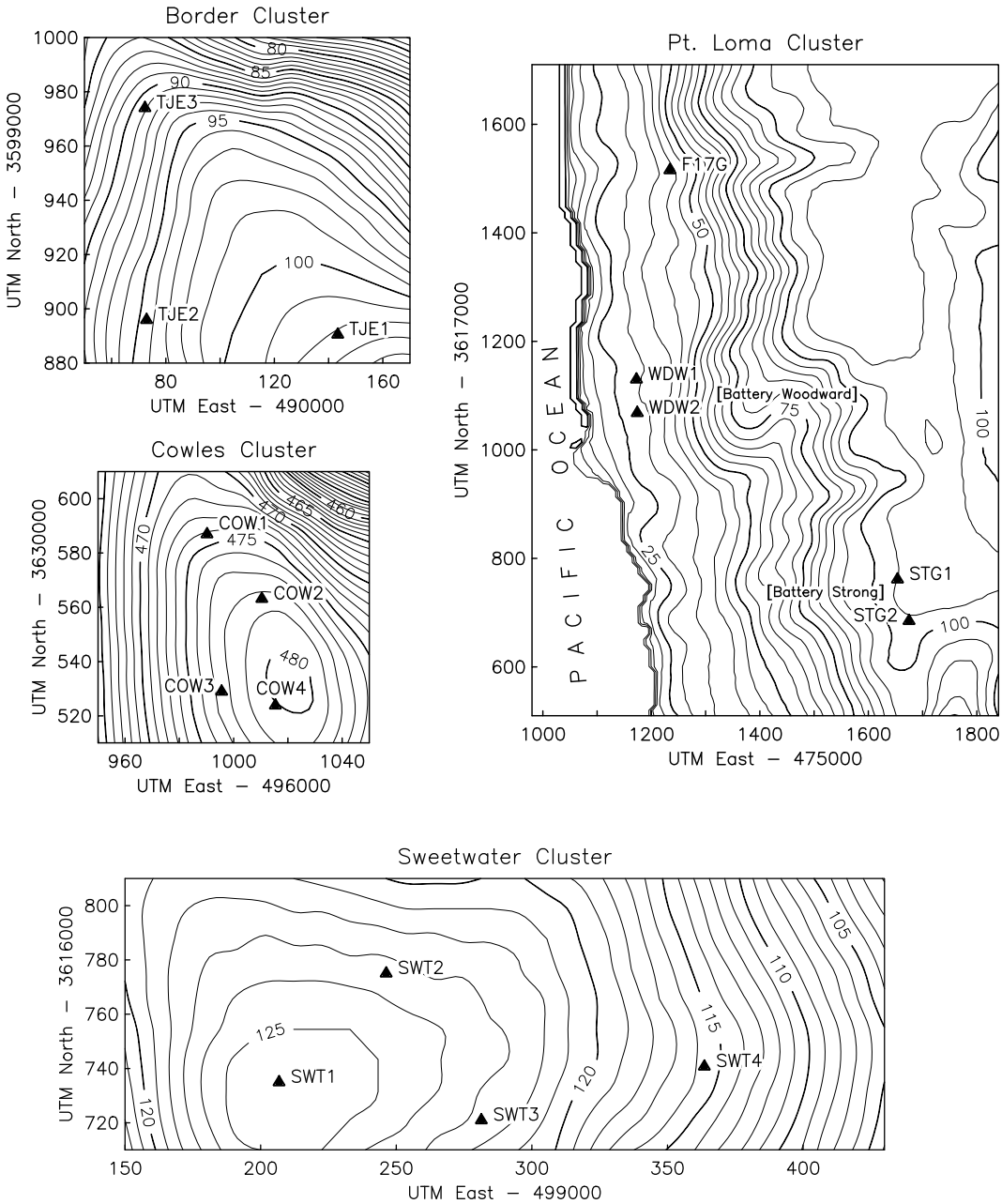

Figure 2

Cowles Mountain (**COW1-4**): We installed four monuments atop this peak, northeast of downtown San Diego and about 12 km east of the Rose Canyon Fault. The monuments are in large rock outcrops. This site is in a regional park and immune to future development; while vehicle access is restricted, the mountain is a popular hiking destination, so equipment cannot be left unattended.

Sweetwater Park (**SWT1-4**): Here we set four monuments on a small hill south of the Sweetwater reservoir, again in large rock outcrops. This is a hiking area and equipment cannot be left unattended.

Point Loma (**WDW1-2, STG1-2, F17G**): Thanks to help from personnel at the Navy SPAWAR facility, which occupies much of Point Loma, we were able to set five monuments in massive concrete structures originally built for coastal artillery (Joyce 1995). Four of the marks are set in the

abandoned gun platforms for Battery Strong (two 8″ guns, built 1938) and Battery Woodward (two 6″ guns, built 1941): each battery had two platforms about 60 m apart. Obviously, these are very large masses of concrete. A fifth mark is set in the outer wall of an underground equipment bunker. Since access is through Navy-controlled checkpoints, and security badges are required, equipment may be left unattended.

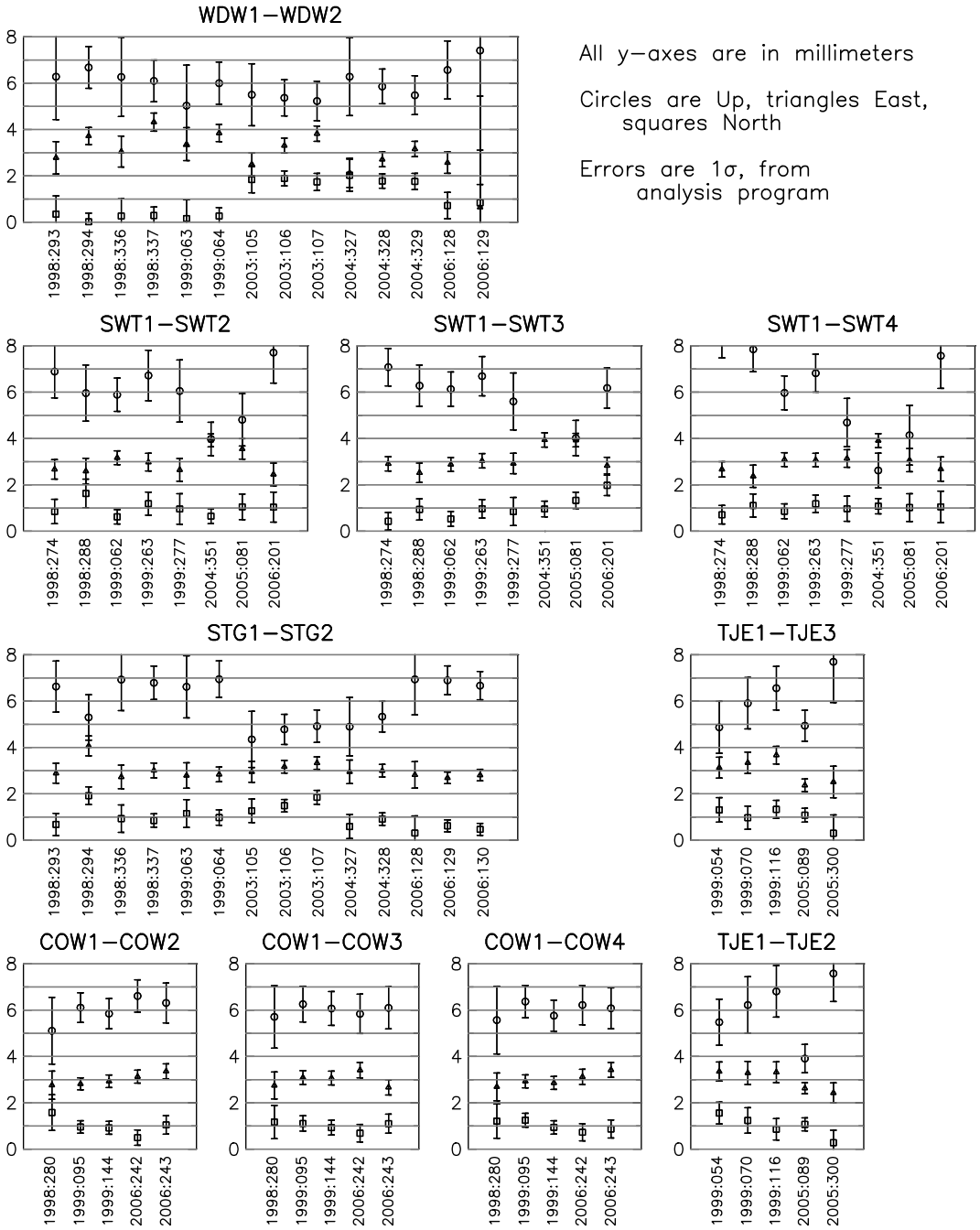

Figure 3

Border State Park **TJE1-3**: Again benefiting from San Diego's past harbor defenses, we set three monuments in the several massive buried concrete structures built as spotter's bunkers ("base-end

stations'') for coast artillery in the early 1940's; these are set in a hill on the border with Mexico, about 1.5 miles from the coast. While the area is heavily patrolled, we have been informed that we should not leave equipment unattended: it would disappear across the border.

Isla Los Coronados, Mexico (**CIS1-3**, not shown in **Figure 2**): After much negotiation, helped substantially by Dr. Javier Gonzales (at CICESE in Ensenada), we were able to install 3 monuments on the largest island, along the ridgeline of the main peak. The marks are about 100 m from each other, and one is within 20 m of the continuous site CORX. The island is controlled by the Mexican Navy who maintain a small base there. Access is either by helicopter or small boat. Equipment can be left unattended.

1.1.4. Repeatability

Of course, the proof of the idea of monument clusters, and of our ability to survey between nearby marks to very high accuracy, lies in the results we have obtained from our surveys. In 1998 and 1999 we surveyed each of the above sites at least three times. The funding from this grant allowed us to make repeat surveys between 2003 and 2006. We started by retraining personnel in the use of the ultraprecise centering methods. The field program began with occupations of the marks on Point Loma, since these will provide the best estimate of motion across the fault. Some time was required to get permissions to revisit some of the marks, in view of increased security concerns both at Point Loma and near the international border. The latter mark cluster was particularly important to repeat because it is likely to be destroyed should a large-scale border fence be constructed. Heavy rains made the road to Cowles Mountain impassable for some time, and we were not able to return to this location until 2006. Logistics have made a re-occupation of the CIS network infeasible.

All surveys used the same equipment (Ashtech Z-12's with choke-ring antennas) as were used in the 1998-99 surveys. Occupation times were at least 6 hours, with at least two independent repetitions. The most repeats were at the Pt. Loma cluster, where the security also allowed longer observation times. All data have been archived at the SCEC Data Center and are publicly available.

We analyzed the data using the L1 and L2 phase independently (an option in the GAMIT software), not solving for separate zenith delays at each site. **Figure 3** shows the results graphically for the shorter baselines, and **Table 1** gives the RMS about the mean and after a weighted fit of a linear trend. The rates and their errors are expressed in μm/yr; most of them are not significantly different from zero.

Table 1: Results for Short Baselines

Line	#	Distance		North				East				Vertical			
		Horiz. m	Vert. m	RMS1 mm	rate μm/yr	error μm/yr	RMS2 mm	RMS1 mm	rate μm/yr	error μm/yr	RMS2 mm	RMS1 mm	rate μm/yr	error μm/yr	RMS2 mm
COW1_COW2	5	31.275	6.418	0.35	−36	43	0.32	0.22	50	37	0.09	0.51	81	94	0.36
COW1_COW3	5	58.312	4.960	0.17	−21	48	0.15	0.27	1	41	0.27	0.20	−18	107	0.21
COW1_COW4	5	68.009	7.539	0.20	−42	45	0.11	0.25	54	40	0.12	0.29	20	103	0.28
STG1_STG2	14	79.361	−0.006	0.47	−61	31	0.44	0.34	−34	31	0.33	0.96	−30	74	0.94
WDW1_WDW2	14	61.659	−0.006	0.76	249	44	0.57	0.88	−144	43	0.76	0.63	−66	105	0.70
SWT1_SWT2	8	56.318	−3.627	0.30	−14	54	0.33	0.48	90	45	0.48	1.10	−188	116	1.17
SWT1_SWT3	7	75.826	−5.066	0.48	143	49	0.21	0.41	83	41	0.35	0.91	−201	103	0.76
SWT1_SWT4	8	156.952	−11.215	0.14	22	53	0.13	0.43	87	45	0.44	1.89	−466	114	1.83
TJE1_TJE2	5	70.667	−7.928	0.43	−56	61	0.35	0.39	−121	54	0.05	1.25	−213	136	1.45
TJE1_TJE3	5	109.630	−10.510	0.37	−42	64	0.32	0.49	−167	58	0.20	1.06	−84	143	1.22

Second column is number of observations; except for the STG and WDW lines these are all independent setups. The RMS values are either about the unweighted mean (RMS1) or a weighted fit of a mean and trend (RMS2).

The results in **Table 1** can be used to bound the levels of random walk and white noise that are present; we expect the former from monument motion and the latter from GPS error and setup error. While maximum likelihood techniques exist to find the noise levels for a single series (Langbein and

Johnson 1997, Williams 2003), these do not give bounds, and also work poorly with the very small numbers of data we have here. We instead adopt a simpler approach that allows us to pool all the results, making the assumption that they can be regarded as having the same noise levels. Certainly an examination of **Table 1** does not suggest otherwise. Pooling the RMS values about the mean for the East and North components gives a total of 20 values, whose empirical cumulative distribution function (CDF) is shown by the black curve in **Figure 4**.

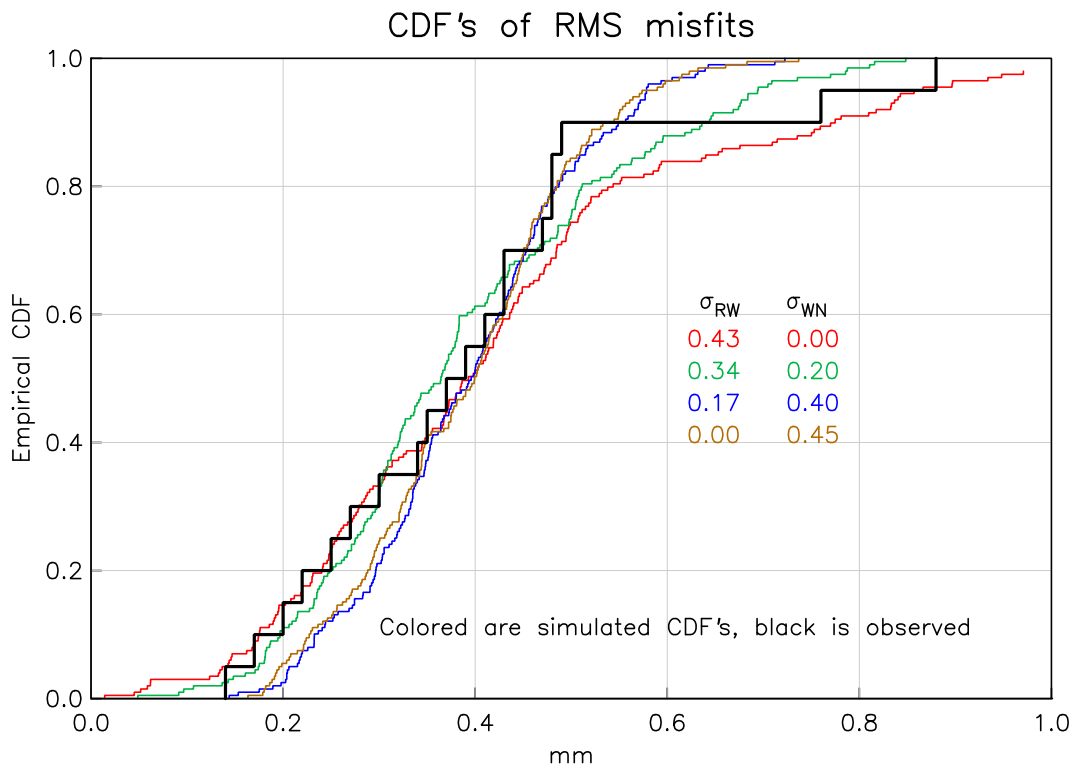

Figure 4

We next construct, using a simple Monte Carlo method, the CDF's expected for different amounts of noise. We construct a very long artificial series which combines random-walk and white-noise components, and compute 20 values of the RMS about the mean, sampling the artificial series just as the real one was sampled, though making the start of each sample is taken randomly within the artificial series. Repeating this a number of times gives a larger set of RMS values whose empirical CDF may be compared with that observed. **Figure 4** shows 4 cases which among them illustrate the range of acceptable values. With no white noise, a σ_{RW} of $0.43\,\mathrm{mm}/\sqrt{\mathrm{yr}}$ gives a similar CDF; the value could be as high as $0.5\,\mathrm{mm}/\sqrt{\mathrm{yr}}$, but not higher. Of course the absence of white noise is not expected, and as this becomes larger the possible upper bound on σ_{RW} decreases; for white noise approaching 0.4 mm the level of random-walk noise could be zero. However, the model with $\sigma_{RW} = 0$ and a white noise of 0.45 mm fits the data only if the larger RMS values are ignored—which may be reasonable, since these all come from a single baseline (WDW1 to WDW2). A plausible value for the white noise (0.2 mm) gives $\sigma_{RW} = 0.3\,\mathrm{mm}/\sqrt{\mathrm{yr}}$: about one quarter the value found by Langbein and Johnson (1997) for pier-type monuments. This lower level, and the redundancy of the network, suggests that we will be able to get adequately precise measurements of motion, though we are still working on how best to combine short and long baselines in order to do this.

1.2. Continuous GPS Data

In parallel with the work described in the previous section, we have analyzed data from the permanent GPS stations operated by the SCIGN and PBO networks. The PBO densified the network in much of San Diego County in early 2005, and the County of San Diego added more stations in early 2006. The PBO plans to install a station on Pt. Loma to replace the existing Coast Guard site (PLO3, mounted on a tower), but is still in the process of obtaining permission. Unfortunately, the SCIGN station on the Coronados Islands (CORX) failed in 2005 and has not yet been repaired. (This station was installed in 2000, but had very high noise prior to 2003 because of a bad antenna.) All this means that the time series available are all shorter than would be desirable, but it is nevertheless worthwhile to see what they show at this point.

For analyzing the continuous data, we invert the GPS timeseries of displacement produced by SOPAC to determine a time series of strain (and network displacement) assuming that the strain within a network is homogeneous. This can be done for any network of three or more sites; for more than three the problem is overdetermined.

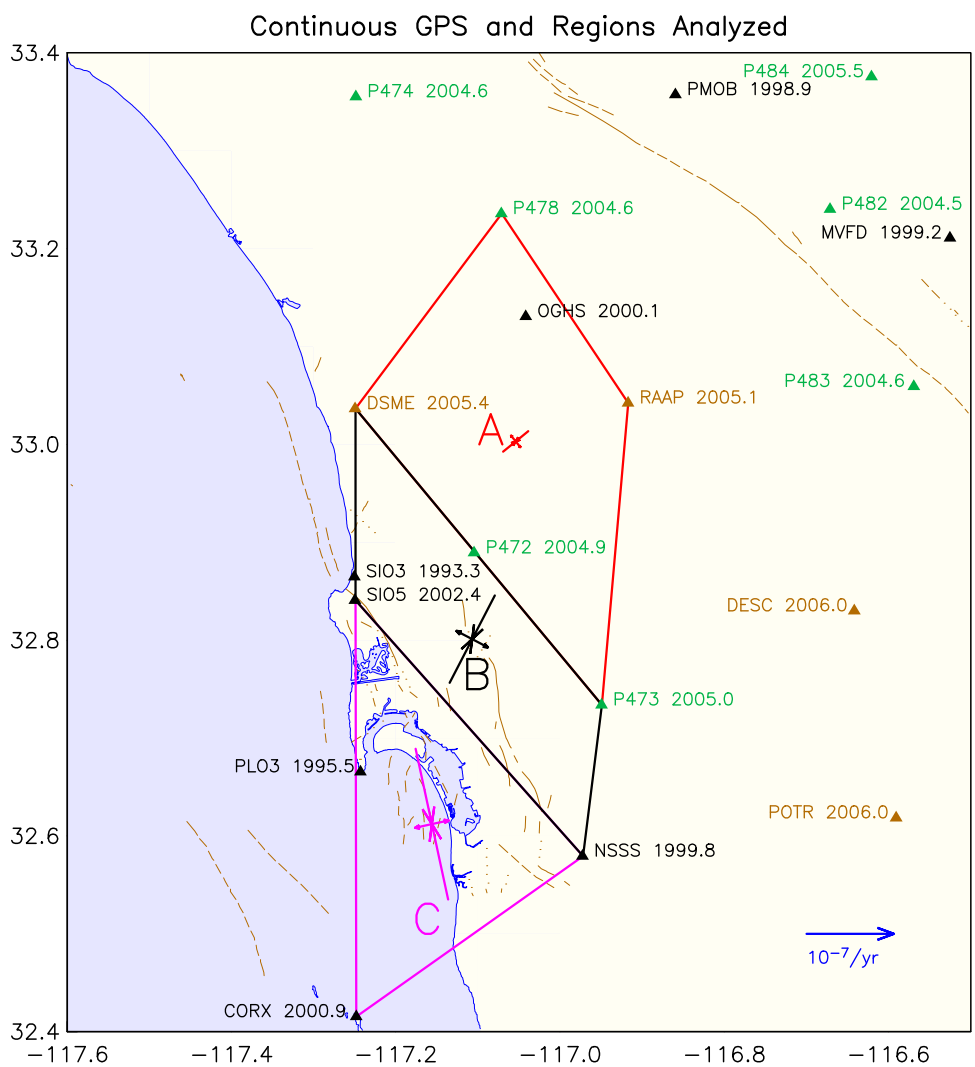

Figure 5

Figure 5 shows three networks within San Diego County (and offshore) along with the locations of all current continuous stations, with the dates at which they began operations. Black is SCIGN, green PBO, and brown San Diego County. The networks have been chosen to provide a maximal length of time with all stations in operation, and also to cover what might be expected to be different areas: A is far from both the Elsinore and Rose Canyon fault zones, B is closer to the Rose Canyon, and C straddles it. The strain analysis included all stations within each polygon, except that SIO3 was not used because of obvious weather-related motion from the heavy rains of early 2005.

Table 2: Regional Strain Rates

Rate	Region		
	A	B	C
$\frac{1}{2}(\dot{e}_{11}+\dot{e}_{22})$	−0.005	−0.018	−0.034
$\dot{e}_{12}$	−0.013	−0.031	0.022
$\frac{1}{2}(\dot{e}_{11}-\dot{e}_{22})$	−0.003	0.022	0.049
θ	−51°	−27°	12°
$\dot{e}_1$	0.009	0.020	0.020
$\dot{e}_2$	−0.019	−0.056	−0.087

Strain rate unit is in 10^{-6}/yr. θ is angle (counterclockwise from East) of the principal strain rate $\dot{e}_1$.

Figure 6 shows the shear and areal strain time series for each network: because of the failure of the CORX station, and the recent start dates of the others, none of these series are very long. **Table 2** gives the strain rates derived by fitting a trend to the time series; **Figure 5** shows the rates as principal strains.

Given the relatively short span of data available, it is encouraging that the pattern of strains is at least both coherent, and consistent with expectations to the extent that the strain decreases as we move to the northeast. The actual pattern of strain—nearly pure north-south contraction—would be consistent with right-lateral shear at 45° plus areal contraction. Without more detailed modeling of the strains expected from the actual fault geometry, it remains unclear how much of the pattern seen can be attributed to strain accumulation from the Rose Canyon fault alone.

1.3. Other Activities

Finally, a contribution of this project to other measurements was the construction of a set of precise-centering antenna mounts for the Caltech Tectonic Observatory for use in Indonesia. This was done at no expense to this grant, but benefited from the design effort that it had supported.

References

H. Johnson and D. Agnew, "Monument motion and measurements of crustal velocities," *Geophys. Res. Lett.,* 22, pp. 2905-2908 (1995).

Barry A. Joyce, *A Harbor Worth Defending: A Military History of Point Loma,* Cabrillo Historical Association, San Diego (1995).

J. O. Langbein and H. Johnson, "Correlated errors in geodetic time series: Implications for time-dependent deformation," *J. Geophys. Res.,* 102, pp. 591-603 (1997).

A. L. Mao, C. G. A. Harrison, and T. H. Dixon, "Noise in GPS coordinate time series," *J. Geophys. Res.,* 104, pp. 2797-2816 (1999).

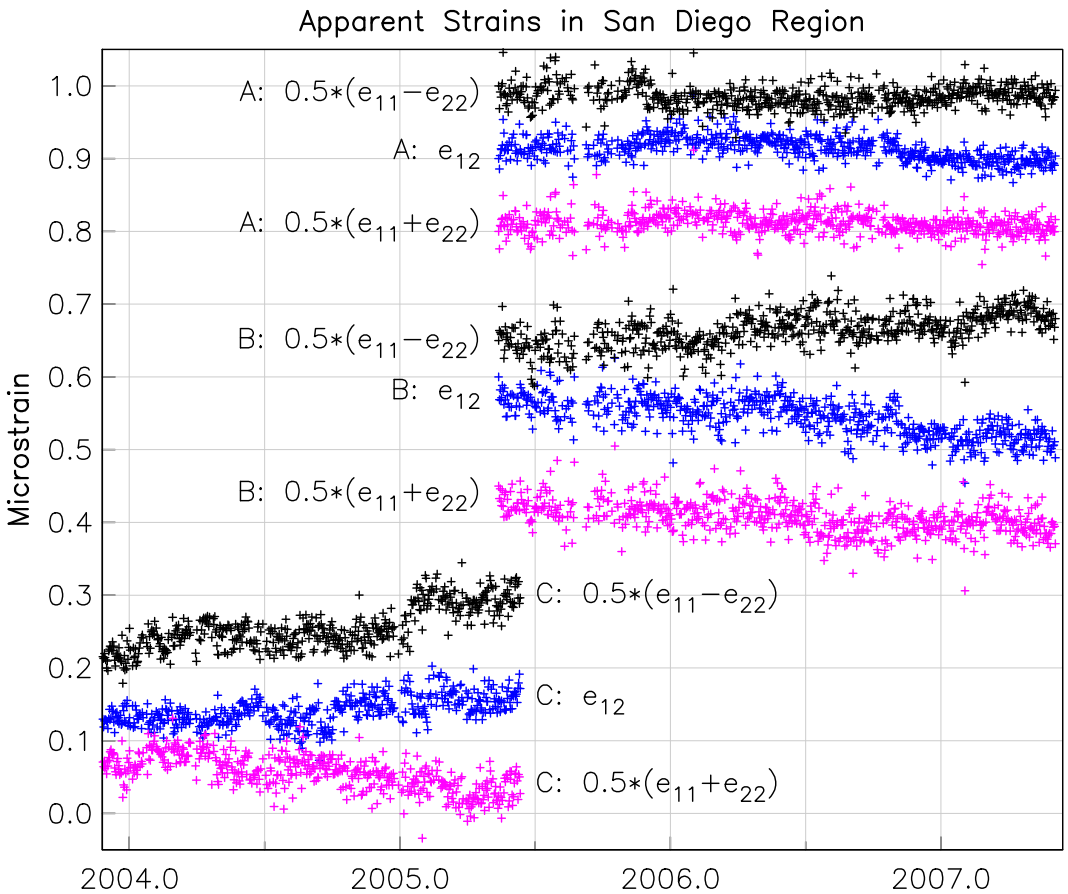

Figure 6

S. D. P. Williams, "The effect of coloured noise on the uncertainties of rates estimated from geodetic time series," *J. Geod.,* 76, pp. 483-494 (2003).

J. Zhang, Y. Bock, H. Johnson, P. Fang, J. Genrich, S. Williams, S. Wdowinski, and J. Behr, "Southern California Permanent GPS Geodetic Array: Error analysis of daily position estimates and site velocities," *J. Geophys. Res.,* 102, pp. 18035-18055 (1997).

Bibliography

Papers describing the precise-centering equipment and the results over short baselines, and giving the results from the surveys and continuous GPS data, are in preparation.